Dissolved organic matter in urban forestland soil and its interactions with typical heavy metals: a case of Daxing District, Beijing

Chen Zhao, Shi-Jie Gao, Lei Zhou, Xiang Li, Xi Chen & Chong-Chen Wang

Environmental Science and Pollution Research

ISSN 0944-1344
Volume 26
Number 3

Environ Sci Pollut Res (2019)
26:2960-2973
DOI 10.1007/s11356-018-3860-7

Springer

Environmental Science and Pollution Research (2019) 26:2960–2973
https://doi.org/10.1007/s11356-018-3860-7

RESEARCH ARTICLE

Dissolved organic matter in urban forestland soil and its interactions with typical heavy metals: a case of Daxing District, Beijing

Chen Zhao[1] · Shi-Jie Gao[1,2] · Lei Zhou[1] · Xiang Li[1] · Xi Chen[1] · Chong-Chen Wang[1]

Received: 28 September 2018 / Accepted: 26 November 2018 / Published online: 30 November 2018

Abstract

As an active substance, dissolved organic matter (DOM) acts a pivotal part in heavy metals (HMs) transportation from urban forestland soil to aquatic ecosystem. In this study, the soil samples from 35 individual subareas were scientifically collected with the aid of geographical information system (GIS) technology. UV-visible (UV-vis) and excitation-emission matrix (EEM)–related parameters suggested that the DOM in urban forestland soil mainly originated from terrestrial and microbial sources. Fluorescence quenching titration associated with parallel factor (PARAFAC) modeling was applied to quantify the complexation ability of four HMs (Cu, Cd, Pb, and Ni) and DOM in urban forestland soil. One fulvic-like (C1), two humic-like (C2 and C3), and one protein-like fluorophores (C4) were identified by EEM-PARAFAC modeling. Considerable differences in fluorescence quenching curves were observed between individual organic constituents and target HMs. Among the four HMs, addition of Cu(II) ions resulted in EEM spectra quenching of each PARAFAC-decomposed organic constituent. However, relatively strong fluorescence quenching phenomena were only detected in humic-like constituents (C2 and C3) with the titration of Pb(II) and Ni(II), which revealed that these types of organic constituent were predominantly responsible for Pb(II) and Ni(II) binding in urban forestland soil–derived DOM. Furthermore, considering the resistant nature of C2 and C3 constituents along with their significant quenching effects for the four target HMs, the concentrations of humic-like constituents in urban forestland soil may be a useful parameter to evaluate the potential risk of HMs immobilization and transformation.

Keywords Urban forestland soil · Dissolved organic matter · Characterization · Heavy metal · Quenching · EEM-PARAFAC

Introduction

Urban forest acts a significant part in enhancing the quality of the natural environment. Well-managed urban forests can reduce stormwater runoff, relieve the pressure of the heat island, sequestrate CO_2, and reduce air pollution (Yang et al. 2005). As the political, economic, and cultural center of China, Beijing has experienced fast-speed urbanization and industrialization in the past few decades. The rapid development has put large amounts of pressure on its ecological environment. Heavy metal (HM) pollution is the critical issue, particularly in the urban forestland soil, which might originate from numerous anthropogenic activities like energy manufacturing (Al-Khashman and Shawabkeh 2006; Kumar et al. 2008), architecture industry (Ye et al. 2011), automobile exhaust (Ward et al. 1977; Wei and Yang 2010), waste disposal (Luo et al. 2011) and fuel combustion (Lind et al. 1999; Meza-Figueroa et al. 2007). The above activities discharge HMs into the air and they subsequently are accumulated into urban forestland soil as the HM-containing dry precipitation.

Dissolved organic matter (DOM) in soil ecosystems is a small but active part, which can interact with HMs to generate metal-organic complexes, thus exerting important influences on their morphology, distribution, biological toxicity, transportation, and transformation (Kalbitz and Wennrich 1998; Weng et al. 2002). In particular, the binding affinity of DOM with HMs can dramatically affect the soil quality, and also the

Responsible editor: Zhihong Xu

Electronic supplementary material The online version of this article (https://doi.org/10.1007/s11356-018-3860-7) contains supplementary material, which is available to authorized users.

✉ Chong-Chen Wang
chongchenwang@126.com

[1] Beijing Key Laboratory of Functional Materials for Building Structure and Environment Remediation, Beijing University of Civil Engineering and Architecture, Beijing 100044, China

[2] College of Forestry, Beijing Forestry University, Beijing 100083, China

mobilization and migration of HMs towards the aquatic environments (Ashworth and Alloway 2004; Refaey et al. 2017; Sun et al. 2017). Therefore, investigations on the interaction mechanism between HMs and DOM were significant to clarify the biochemical cycling of HMs in urban forestland soil environments.

The binding characteristics of HM-DOM were strongly related to the organic sources, compositions, and structures. For example, the humic-like and protein-like components extracted from municipal solid waste leachate were responsible for Cu(II) binding; whereas the protein-like component was the only fraction involved in Cd(II) complexation (Wu et al. 2012). Comparing with the Cu(II) ions, Zn(II) ions showed a lower affinity to DOM derived from lake sediments (Xu et al. 2013). Typically, phenolic hydroxyl and carboxylic ligands within DOM compositions were typically regarded as powerful and weak HMs binding sites, respectively (Croué et al. 2003; Hur and Lee 2011). Previous studies had verified that the capacities of DOM to bind HMs during their migration through the soil were one element that may prominently affect the quality of water environments. Because of the generation of resistant, aqueous complexes with HMs, such as Cu, Pb, and Hg, DOM can strengthen metal mobilization and transportation towards the groundwater (Ashworth and Alloway 2004; Dudal et al. 2005). Wu et al. (2003) suggested that some small organic acids (average molecular weight < 500 Da) in agricultural soil, such as acetic, oxalic, malic, and citric, can generate stable complexes with HMs. Yang et al. (2006) also found that massive small molecules of organic acids can affect the adsorption-desorption equilibrium of Pb in acidic clayey soil. Recently, researchers paid more attention to explore the effects of remediation materials (sewage sludge compost, food waste compost, biochars, etc.) on soil organic substances, revealing that they remarkably modified the chemical properties of DOM and subsequently influence the mobility and bioaccumulation of HMs (Beiyuan et al. 2018; Fang et al. 2016; Li et al. 2018a). However, up to now, few attentions were carried out to characterize the DOM in urban forestland soil and study its binding properties with co-existing HMs.

UV-visible (UV-vis) and excitation-emission matrix (EEM) spectroscopies are user-friendly, rapid, and non-destructive instruments that can supply useful information about the chemical compositions and molecular structures of DOM (Wang et al. 2018a; Zhao et al. 2015; Zhao et al. 2016; Zhao et al. 2018b). More specifically, EEM spectra combined with quenching analysis had been proven to be a reliable method to explore the interaction mechanism between HMs and organic substances (Chen et al. 2013; Yamashita and Jaffé 2008; Zhu et al. 2014). Introduction of parallel factor (PARAFAC) modeling to EEM spectroscopy can cut down the interference of overlapping peaks in original fluorescence spectra, obtain the binding parameters between metal ions and individual fluorophores in DOM, and provide much more quantitative and specific information (Huang et al. 2018; Wang et al. 2018b; Wang et al. 2016; Wu et al. 2011; Wu et al. 2012). Ohno et al. (2008) verified that the binding characteristics between water soluble soil organic matter (WSOC) and trivalent metals (Fe and Al) might be well analyzed by EEM-PARAFAC modeling. Moreover, Xu et al. (2013) successfully estimated the binding characteristics of lake sediment–derived DOM and divalent metals (Zn and Cu) with the identical method.

In this study, field experiments were conducted in Daxing District, which is the largest region in southeast of Beijing, China. To make the subsequent analysis more representative and systematic, the sampling work was completed under the aid of geographical information system (GIS) technology. The objectives were (1) to use UV-vis and EEM spectroscopies to evaluate the chemical compositions and structures of DOM extracted from urban forestland soil in Daxing District; (2) to investigate the feasibility of EEM-PARAFAC and quenching method for application in quantification of the binding characteristics of HMs and DOM in forestland soil. Based on the above purpose, Cu, Cd, Pb, and Ni, which have comparatively high concentrations and biotoxicity in soil in Beijing (Chen et al. 2010), were selected as the representatives to discuss. Finally, this study may offer an in-depth view of the heterogeneous properties of HMs complexing to DOM existed in urban forestland soil at the molecular level and the influences of DOM on the environmental behaviors and the ecological risk of HMs in the soil ecosystems.

Materials and methods

Reagents and instruments

All chemical reagents were analytical grade from J&K Chemical Corporation (Beijing, China) and were used directly without any further purification. Each of the experimental solution was prepared with ultrapure water of resistance not less than 18.2 MΩ cm^{-1}. The contents of the four heavy metal titrants were standardized with the EDTA solution (Bai et al. 2008).

The pH values of the forestland soil samples were determined in a suspension (the ratio of water to dry soil was 2.5) utilizing a PB-10 pH meter (Sartorius, Germany). The total N and P of the soil samples were detected applying an AA3 continuous-flow analyzer (Seal Analytical Corporation, Germany). The HMs and dissolved organic carbon (DOC) contents in the extracted samples were measured by a Perkin-Elmer AA-PinAAcle 900 atomic absorption spectroscopy (Fermont, USA) and a Jena multi N/C 3100 analyzer (Jena, Germany), respectively. UV-vis and EEM spectra were determined on a Perkin-Elmer lambda 650S spectrophotometer (Fremont, USA) and a Hitachi F-7000 Fluorescence

spectrophotometer (Tokyo, Japan), respectively. Standard quinine sulfate units (QSU) were selected to compare the relative concentrations of fluorophores, in which 1 QSU was equivalent to 32.2 intensity unit. The primary scatters (Rayleigh Raman scatters) were removed by setting zero to the EEM spectra in the two triangle regions ($E_x \leq 0.5\ E_m + 5$ nm and $\geq E_m - 20$ nm) (Stedmon and Bro 2008), and by subtracting the blank spectra (ultrapure water in this study) (Santos et al. 2009), respectively.

Soil sampling and pretreatment

The sampling area of this study was concentrated in the Daxing District, Beijing. The total sampling area was approximately 135.28 km^2. The whole area was divided into 35 typical subareas based on GIS technology, which guaranteed the accuracy of the sampling locations (Fig. 1). Average 5 samples were collected at each sampling subarea using Soil Core Samplers (AMS samplers, USA).

In order to facilitate the transportation and follow-up analysis, the collected soil samples were reserved in polyethylene bags. The soil samples were placed in an oven at 50 °C and dried for 3 days (Del Galdo et al. 2003, Lee et al. 2006; Six et al. 2002). After that, they were filtered through a 2.0-mm sieve to eliminate stones, debris, and other interfering substances. Approximately 20 g soil samples were ground in a mechanical agate grinder until fine particles (< 200 μm) were obtained. Remarkably, DOM constituents were extracted by mixing one part of well-prepared soil sample with four parts of ultrapure water and continuously shaking them for 24 h. The extracts were centrifuged for 10 min at 8000 rpm at 4 °C and passed through a 0.45-μm hydrophilic PVDF Millipore membrane (Nierop et al. 2002; Yu et al. 2012), and the physicochemical parameters of DOM were shown in Table 1.

Fluorescence quenching titration

Prior to fluorescence titration, DOM in extracted solutions with absorbance greater than 0.02 at 350 nm will be diluted with ultrapure water, and the ionic strength of the DOM solutions were controlled by 0.1 mol L^{-1} $KClO_4$ to avoid the inner filter effects (Ohno 2002). The pH values of the solutions were adjusted to the expected values (pH = 4.0 for $Cu(NO_3)_2$, pH = 4.5 for $Pb(NO_3)_2$ and $Ni(NO_3)_2$, pH = 6.0 for $Cd(NO_3)_2$) by adding 0.1 mol L^{-1} HNO_3 or NaOH solutions, and the total addition should not exceed 200 μL. Both aliquots of 25 mL diluted DOM extract and 0.02 mol L^{-1} HM standard solutions were put into 40-mL brown sealed vials. The HM concentrations in the ultimate solutions remained in the range of 0–600 μmol L^{-1} with the content interval of 40 μmol L^{-1}. All mixed solutions of DOM and HMs were shaken for 24 h without light irradiation at ambient temperature to guarantee equilibrium of complexing reactions (Zhao et al. 2018a). In addition, the same volume of DOM solution with the ionic

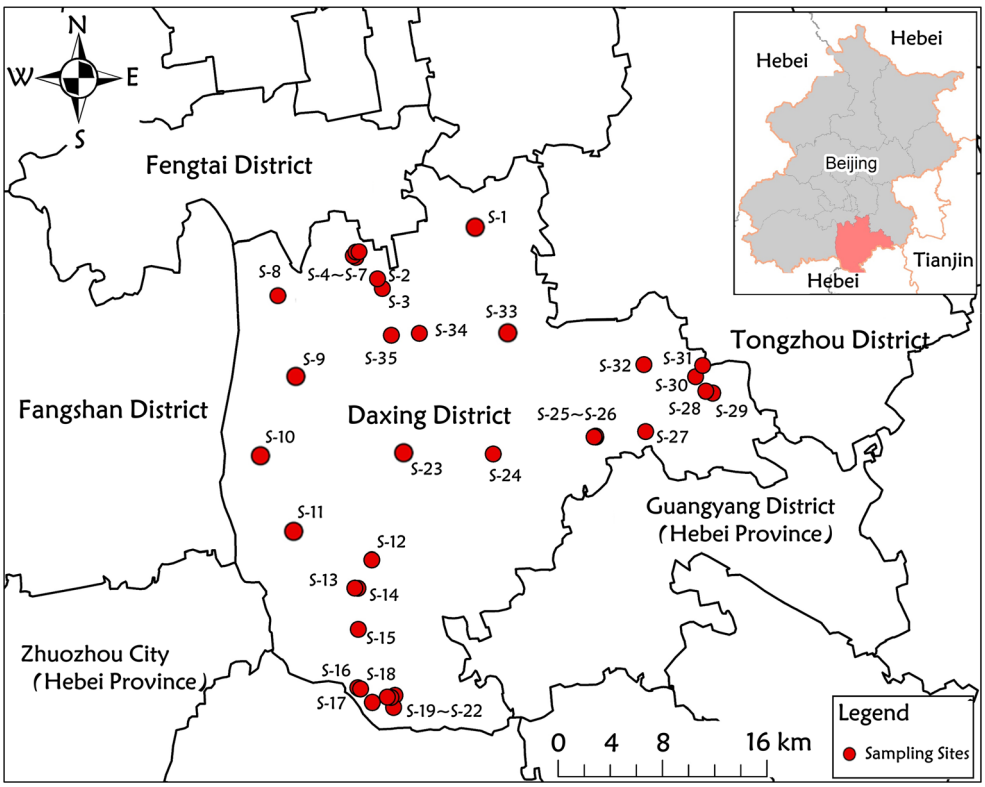

Fig. 1 Schematic map of the target area and the sampling sites

Table 1 Background chemical characteristics of the collected urban forestland soil samples ($n = 35$)

Values	pH	TN g kg^{-1}	TP	TOC mg L^{-1}	Cu μg L^{-1}	Cd	Pb	Ni
Range	6.57–7.80	0.02–0.11	0.05–0.51	3.61–16.85	7.11–27.25	0.51–5.28	0.21–2.88	0.50–14.20
Mean	7.23	0.06	0.21	9.50	13.35	1.86	0.94	5.32
Median	7.43	0.06	0.19	8.69	15.12	1.27	0.83	6.21
RSD (%)	7.12	49.45	70.82	35.56	42.67	37.28	31.07	45.21

strength of 0.1 mol L^{-1} $KClO_4$ was selected as the blank to accomplish EEM fluorescence measurement.

PARAFAC modeling

PARAFAC model can systematically decompose and extract individual organic substances from EEM spectral dataset. It also offers the relative abundance of individual organic constituent in each sample (Ohno et al. 2008; Stedmon and Bro 2008). All EEM spectra data in this study were compiled into three-way arrays of X with $I \times J \times K$, where I, J, K represent the amount of samples, emission, and excitation wavelengths, respectively. The modeling can be described using Eq. (1):

$$X_{ijk} = \sum_{f=1}^{F} a_{if} b_{jf} c_{kf} + \varepsilon_{ijk}\ i = 1, ..., Ij = 1, \ldots, Jk = 1, ..., K \quad (1)$$

where F is the amount of fluorophores, X_{ijk} defines the fluorescent peak of sample i at given emission j/excitation k wavelength; a_{if} is proportional to the content of the f_{th} organic constituent in the i_{th} sample; b_{jf} and c_{kf} are assessments of the emission and excitation spectra, respectively, for the f_{th} organic constituent. Finally, ε_{ijk} defines the residual matrix to minimize the sum of squared residuals by changing least squares algorithm (Stedmon et al. 2003).

EEM-PARAFAC analysis (99 samples × 55 emissions × 55 excitations) was completed applying the DOMFluor toolbox in MATLAB 7.0 software (Mathworks, Natick, MA). The relative concentrations of individual fluorophores were described by maximum fluorescence intensities (F_{max}). Split-half analysis was used to prove the correctness of the decomposed data from PARAFAC modeling.

Complexing reaction modeling

In this research, the Ryan-Weber model was used to quantify the binding parameters between HMs and individual organic constituents decomposed from EEM-PARAFAC modeling, which can provide more accurate and detailed information than the traditional peak maxima method (Ryan and Weber 1982a). The principle of this model assumes that organic ligands complex with HMs at a molar ratio of 1:1, which can be expressed as Eq. (2):

$$I = I_0 + (I_{ML} - I_0)\left(\frac{1}{2K_M C_L}\right) \times \left(1 + K_M C_L + K_M C_M - \sqrt{(1 + K_M C_L + K_M C_M)^2 - 4K_M^2 C_L C_M}\right) \quad (2)$$

where I_0 and I define the fluorescence intensity without the titration and at the HM concentration of C_M, respectively; I_{ML} is the limiting fluorescence intensity; K_M and C_L are the conditional stability constant and binding capacity, respectively (Yamashita and Jaffé 2008). The fraction of the binding fluorescent components (f) was obtained by Eq. (3):

$$f = \frac{(I_0 - I_{ML})}{I_0} \times 100 \quad (3)$$

Results and discussion

Characterization parameters calculated by UV-vis and EEM spectral data

The UV-vis spectra of DOM extracted from urban forestland soil samples at different sampling sites were illustrated in Fig. 2a, b, which increased approximately exponentially with decreasing wavelength. Similar to previous researches (Hong et al. 2014; Jiang et al. 2017), no prominent absorption peaks were found in the UV-vis spectra, only inconspicuous shoulder peaks were detected in the range of 250–300 nm, which could be attributed to presence of conjugated molecular structures ($\pi \rightarrow \pi^*$ electron transitions) in DOM. To gain more information from these spectra about DOM of forestland soil samples, the spectral slope coefficient ($S_{275-295}$, μm^{-1}), specific UV absorbance at 254 nm ($SUVA_{254}$, L mg C^{-1} m^{-1}), the ratio of UV absorbance at 254 and 203 nm ($A_{253/203}$), and absorption coefficient at 355 nm (a_{355}, m^{-1}) were calculated in this study (the corresponding values were shown in Table 2 and their computational details were revealed in Electronic Supplementary Information).

It is apparent that S is one of the important parameters to characterize DOM. However, the validity of its application

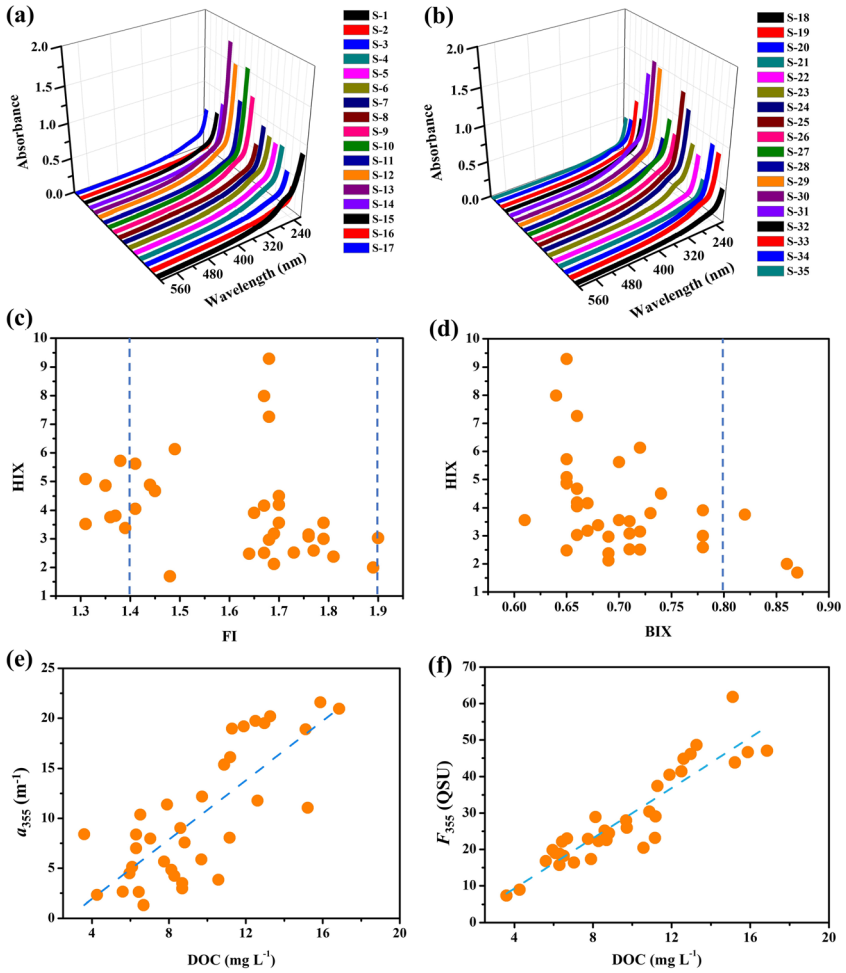

Fig. 2 **a**, **b** UV-vis spectra of DOM extracted from urban forestry soil samples at different sampling sites. **c**, **d** Relationships of FI vs HIX and BIX vs HIX. **e**, **f** Correlations plots between DOC concentrations and CDOM (r^2 = 0.59) and FDOM (r^2 = 0.83)

mainly depends on the calculation range of wavelength. For example, Stedmon et al. (Stedmon and Markager 2001) obtained *S* values by calculating the spectral data from 300 to 650 nm to characterize the DOM in the Greenland Sea. Santos et al. (2012) fitted *S* values within the spectra 240–400 nm to estimate the average molecular weight of DOM in rainwater. In this study, wavelengths between 275 to 295 nm were chosen to calculate the *S* values due to relatively high absorbance levels in this wavelength range. Furthermore, the $S_{275–295}$ has been proven to negatively correlate with the molecular weight of organic substances (Helms et al. 2008). The $S_{275–295}$ values determined for the DOM extracted from urban forestland soil samples were in the range of 12.11–16.20 μm^{-1} with the median of 13.66 μm^{-1}, which were higher than those reported for the other soil organic substances (as shown in Table 3), suggesting that the DOM in the urban forestry soil collected from the above sampling sites had smaller molecular weight. In addition, Spencer et al. (2012) found that the $S_{275–295}$ values could negatively correlate with the hydrophobic organic components, so the hydrophobicity of DOM in the urban forestland soil was weaker than the other soil ecosystems.

$SUVA_{254}$ has been diffusely applied to evaluate the aromaticity of DOM; as illustrated in Table 2, the $SUVA_{254}$values of DOM were in the range of 2.83–6.81 L mg C^{-1} m^{-1} with the

Table 2 DOM optical properties of the collected urban forestland soil samples (n = 35)

Values	$S_{275–295}$ μm^{-1}	$SUVA_{254}$ L mg C^{-1} m^{-1}	$A_{253/203}$	a_{355} m^{-1}	F_{355} QSU	FI	HIX	BIX
Min	12.11	2.83	0.09	1.31	7.33	1.31	1.69	0.61
Max	16.20	6.81	0.27	21.60	61.80	1.90	9.29	0.87
Mean	13.79	4.69	0.19	10.09	28.23	1.72	4.02	0.70
Median	13.66	4.88	0.18	8.38	23.15	1.70	3.56	0.69

Table 3 Summary of UV absorption related parameters of DOM in typical soil environments

Samples	$S_{275–295}$ μm^{-1}	References	Samples	$SUVA_{254}$ L mg C^{-1} m^{-1}	References
Urban forestland soil	12.11–16.20	This study	Urban forestland soil	2.83–6.81	This study
Soil leachate	11.20	(Yang et al. 2015)	Fluvic hypercalcaric cambisol	1.50–3.00	(Hassouna et al. 2012)
Boreal forest soil	11.01–12.84	(O'Donnell et al. 2016)	Grassland soil	1.36	(Stumpe and Marschner 2010)
Permafrost	10.80–15.20	(Gao et al. 2018)	Boreal forest soil	< 4.50	(O'Donnell et al. 2016)
Farmland soil	13.00–16.00	(Jiang et al. 2012)	Saline-alkali soil	< 2.83	(Li et al. 2017)

median value of 4.88 L mg C^{-1} m^{-1}. Being compared to the previous studies about DOM in the other types of soil environments (as shown in Table 3), the corresponding higher $SUVA_{254}$ values demonstrated that much more aromatic substances present in the urban forestland soil samples. The $A_{253/203}$ can offer further information about substituted degree of aromatic DOM structures. Unsubstituted aromatic ring structures typically exhibit a relatively lower value of $A_{253/203}$, and an increase of $A_{253/203}$ value suggests the organic components contain more polar functional groups (i.e., carboxylic, carbonyl, hydroxyl, and ester groups) on aromatic rings (Korshin et al. 1997). The median value of $A_{253/203}$ (0.18) was slightly higher than commercial soil fulvic acids Waskish Peat (0.16) and Pony Lake (0.11) from the International Humic Substance Society (IHSS) (Mignone et al. 2012), implying that DOM in urban forestry soil contained more substitute functional groups and aliphatic chain structures.

In order to further reveal the DOM characteristics, three fluorescent indices, namely the fluorescence index (FI), the humification index (HIX), and the biological index (BIX), were calculated in this study (the corresponding computational details were shown in Electronic Supplementary Information). Among the above three indices, FI can be applied to identify DOM sources, such as autochthonous (> 1.9) and allochthonous sources (< 1.4) (Huguet et al. 2009; Mcknight et al. 2001). As illustrated in Fig. 2e, the FI values of most urban forestland soil samples were between 1.4 and 1.9, suggesting that the DOM might originate from both terrestrial and microbially derived organic substances. Additionally, some of soil samples that exhibited their FI values were less than 1.4, which may be ascribed to great anthropogenic activities. HIX values generally increase as biomass decomposition (Hunt and Ohno 2007), while low HIX values (< 10) indicate that the non-humified structures were dominated in organic components (Huguet et al. 2009). Table 2 showed that the DOM samples from different sampling sites had low HIX values, ranging from 1.69 to 9.29 (Table 2), suggesting that the humification degree of DOM in urban forestland soil was relatively lower, which could be interpreted by two potential reasons: (1) the afforestation time was short (generally less than 10 years), the DOM mainly originated from incomplete decomposition of plant litter, soil humus or root exudates; (2) a massive microorganic production caused by human activities (protein and sugar) might lead to "priming effect," which could stimulate the microbial community to degrade humified organic substances (Bianchi 2011). BIX is a proxy of autochthonous microbially produced DOM inputs (Huguet et al. 2009). The BIX with a high value (> 0.8) represents prominent autochthonous sources of freshly generated organics (Huguet et al. 2009; Huguet et al. 2010). All BIX values in this research varied from 0.61 to 0.87, with the median value of 0.69. This result indicated that most of organic substances in urban forestry soil were terrestrial sources.

The parameters a_{355} and F_{355} were considered as two quantitative indicators of chromophoric DOM (CDOM) and fluorescence DOM (FDOM), respectively (Chen et al. 2004; Guo et al. 2007; Li and Hur 2017). The a_{355} varied from 1.31 to 21.60 m^{-1}, and the F_{355} varied from 7.33 to 61.80 QSU. Both a_{355} and F_{355} correlated positively with DOC concentrations (as illustrated in Fig. 2e, f), revealing that CDOM and FDOM were significant and substantial constituents to the dissolved organic pool in urban forestland soil (Jiang et al. 2017; Zhao et al. 2015). Moreover, a_{355} and F_{355} could be applied as indicators for DOC concentrations via in situ detection in this type of soil ecosystem.

PARAFAC analysis of urban forestland soil DOM

All the fluorescence spectral data of the urban forestland soil samples titrated with four HMs were decomposed by the PARAFAC modeling (Fig. 3). Four organic constituents were distinguished by the PARAFAC from the urban forestland soil DOM, including one fulvic-like constituent (C1), two humic-like constituents (C2 and C3) and one protein-like constituent (C4).

C1 presented one peak at Ex/Em wavelength of 260/450 nm (Fig. 1a, e). This spectral feature was considered as the fulvic-like fluorescence, consistent with previous researches (Liu et al. 2017; Mounier et al. 2011; Zhou et al. 2014). C2 showed a dominating and a secondary peaks at 230/423 nm (Ex/Em) and 315/423 (Ex/Em), respectively. This constituent was similar to the humic acid fluorophores and termed peak C by Coble (1996). C1 and C2 are mainly derived from terrestrial organic precursors like soil extracts, forested streams, wetlands, and deciduous leaves (Fellman et al. 2008; Fellman et al. 2009;

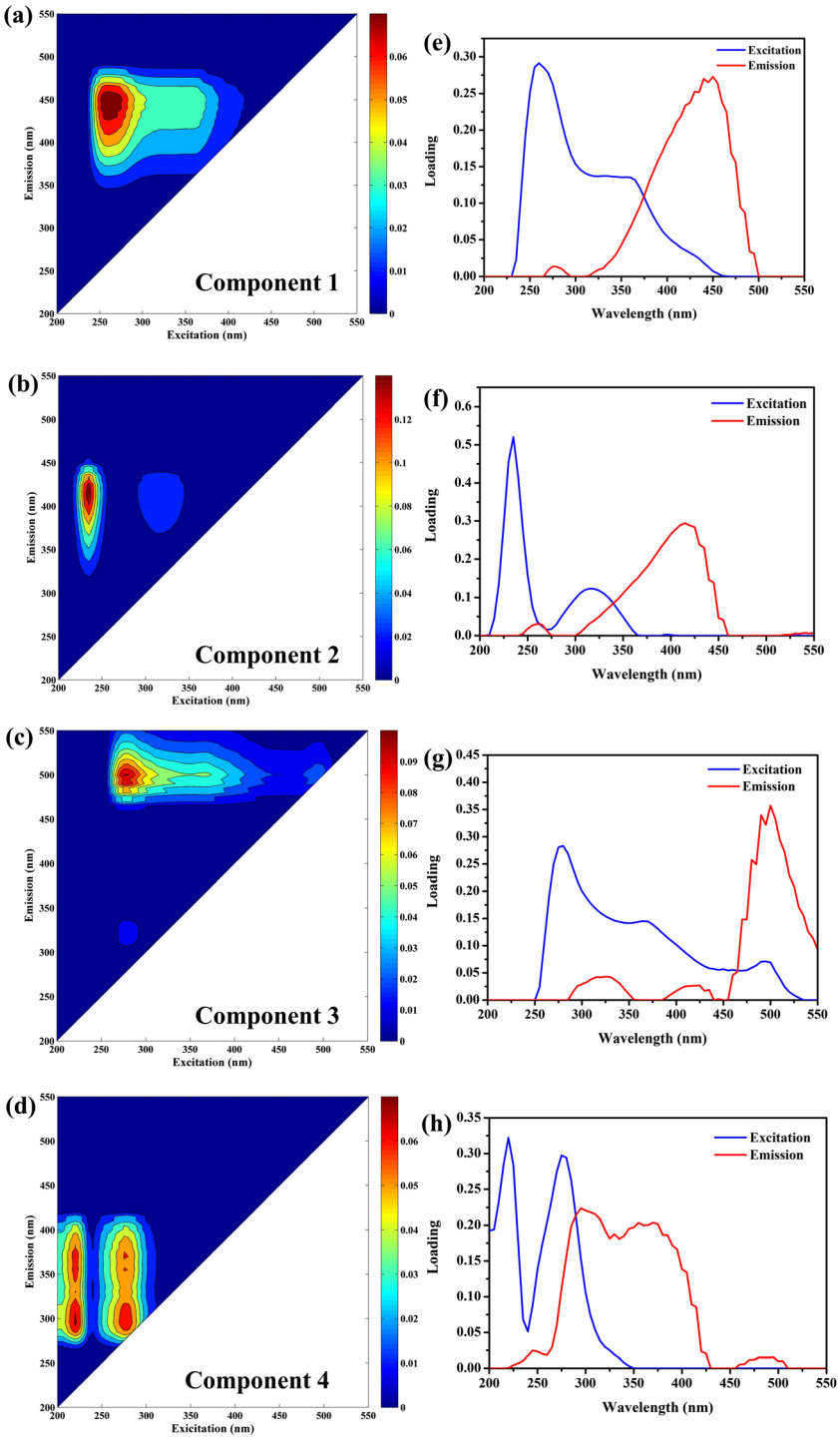

Fig. 3 EEM fluorophores decomposed by PARAFAC model from the urban forestland soil DOM

Stedmon and Markager 2005; Stedmon et al. 2003). Wet precipitation generally leads to an increase in C1 and C2, which can be ascribed to enhancive land-based inputs from stormwater runoff (Stedmon and Markager 2005). It is noteworthy that Ishii and co-workers (Ishii and Boyer 2012) had classified the C1 and C2 constituents as the UVC humic–like constituents based on their peak excitation wavelengths and representative spectra. In view of the limitation of UVC light sources, C1 and C2 identified in this study were expected to be relatively resistant to photodegradation. In addition, Ohno et al. (2010) found that the molecular weight of C1 and C2 constituents in soil ecosystems was much more lower than the other coexisting organic constituents, and the average molecular weight was generally less than 665 Da.

The EEM spectral characteristics of C3 exhibited its peak at 275/500 nm (Ex/Em), which were an integration of terrestrial humic–like fluorescence peak A and peak C (Coble 1996). Lee et al. (2015) reported that fluorophores at short wavelengths were related to the existence of low aromatic organic constituents, while fluorescent organic constituent at long wavelengths were associated with high aromatic polycondensation structural organics. Being compared to C1 and C2, the peak location of C3 was shifted to longer wavelengths. Thus, among the three identified humic-like constituents, C3 organic constituent was probably associated with the highly condensed structures and larger molecular weight, indicating a relatively more refractory and mature nature.

C4 had its maximum at 225/300, 225/375, 275/300, and 275/375 nm (Ex/Em), respectively. The bottom two peaks (225/300 and 275/300 nm) in the EEM spectrum (Fig. 3d) represented tyrosine-like peak B constituents (Coble 1996; Li et al. 2018b; Zhou et al. 2016). The other two peaks (225/375 and 275/375 nm) were attributed to tryptophan-like peak T constituents (Coble 1996; Li et al. 2018b), which were frequently detected in the aquatic environments affected by anthropogenic input (Hong et al. 2012; Phong and Hur 2015). The results suggested that the DOM in urban forestland soil samples contained almost all types of dissolved amino acids (tyrosine- and tryptophan-like constituents), and its chemical composition was susceptible to human activities.

PARAFAC modeling offered excess quantitative information depicting the percentage composition of the fluorophores in the urban forestland soil samples. By calculating the F_{max} values, the DOM displayed the higher abundance of C1 (26.69–47.59%) and C2 (29.44–41.12%), followed by C3 (12.62–23.18%) and C4 (5.80–19.94%). The total F_{max} value of C2 and C3 occupied a predominant proportion in the total organic constituents, indicating that the humic-like organic constituents were the primary sources of the urban forestland soil in Daxing district.

Interactions of PARAFAC-derived constituents with the HMs

The EEM quenching curves of individual constituent with the titration of Cu(II), Cd(II), Ni(II), and Pb(II) were illustrated in Fig. 4. For all fluorophores, a distinct quenching phenomenon was detected for Cu(II), while negligible quenching

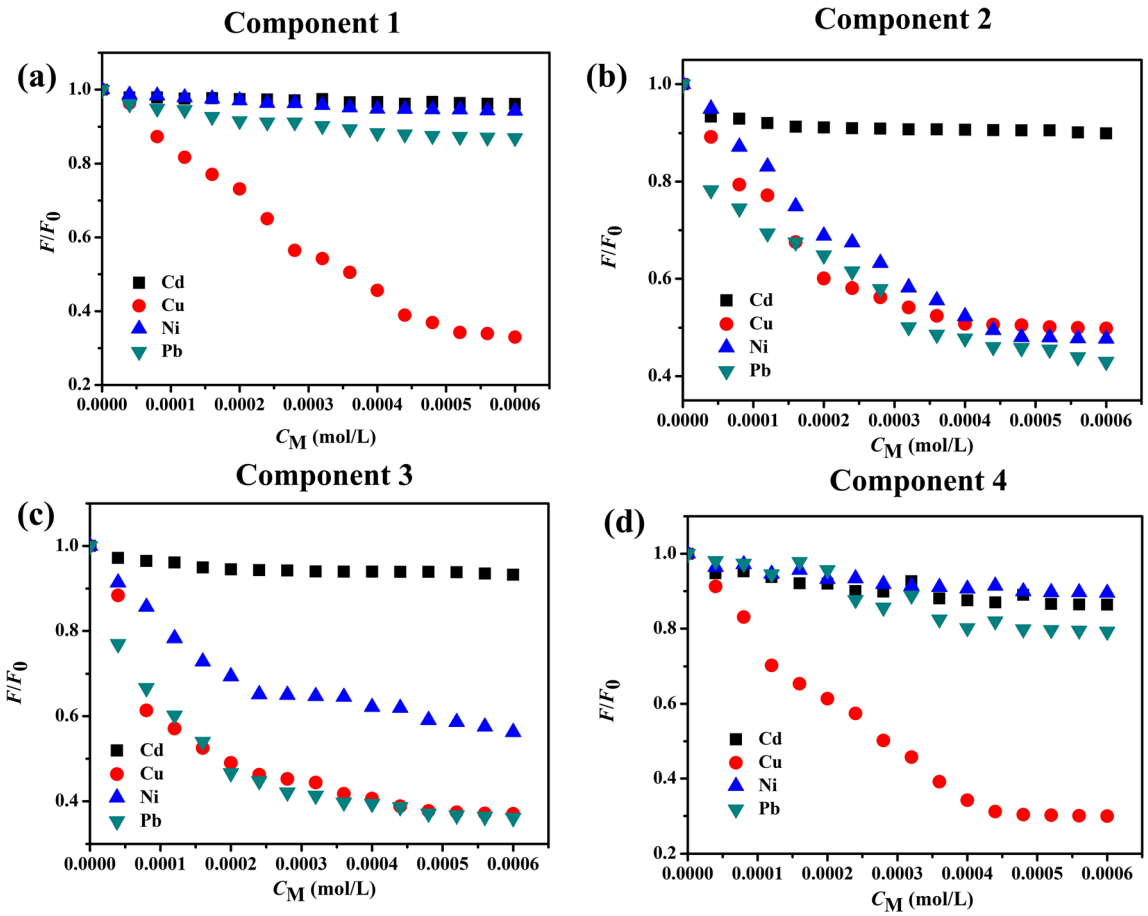

Fig. 4 Variation in the relative fluorescent intensity of individual PARAFAC-derived fluorophores with the addition of Cu(II), Cd(II), Pb(II), and Ni(II) solutions

phenomenon was detected for Cd(II), which were extremely similar to the widespread DOM in aquatic environments (Yamashita and Jaffé 2008), municipal solid waste leachate DOM (Wu et al. 2011), and commercial humic acid (Divya et al. 2009). Interestingly, the titration of Ni(II) and Pb(II) ions had comparatively strong quenching effects on C2 and C3, whereas the quenching effects on C1 and C4 was relatively weak. Weng et al. (2002) applied WHAM model to predict the affinity of sandy soil DOM for heavy metals, following the order: Co < Ni < Cd~Zn < < Pb~Cu. The contradictory results of this study can be attributed to the differences in the functional group, molecular weight, and chemical composition of DOM in urban forestland soil. Previous studies had demonstrated that ligands such as phenols (–OH), amines (–NH_2), and carboxyl (–COOH) may act a significant role in the complexing reaction (Struthers et al. 2008), and HMs with high binding strength were distributed more in the larger DOM fractions (Wu et al. 2004). Therefore, C2 and C3 contained much more active groups that can coordinate with HMs. Moreover, Jordan et al. (1997) concluded that peat-derived humic acid had higher affinity than fulvic acid for Pb, which further verified the accuracy of the PARAFAC model for the classification of four organic constituents in urban forestland soil samples.

With respect to protein-like fluorophores, the complex reaction with HMs might enhance or quench their fluorescent intensities (Wu et al. 2011; Yamashita and Jaffé 2008). Recently, EEM quenching method is diffusely applied to quantify the binding properties between humic-like substances and HMs and has seldom been used to determine the HMs binding parameters of given protein-like or amino acid molecules. Being compared to those of C1–C3, obvious fluctuations were examined in the quenching curves of C4, especially for Cd(II), Ni(II), and Pb(II) ions. This phenomenon can be proved by previous researches that humic-like and protein-like constituents can potentially generate supramolecular assemblies by means of π-π interactions, van der Waals forces, and the other weak dispersive forces (Peuravuori and Pihlaja 2004; Romera-Castillo et al. 2014; Wang et al. 2015). Hence, the enhancement of fluorescent intensities after the complexation of protein-like constituents with HMs was largely attributed to metal-induced steric hindrance, which resulted in the reduction of interaction between protein-like and humic-like constituents (Yamashita and Jaffé 2008). In this research, the fluorescent intensities of C4 were strongly quenched by Cu(II) ions without any fluctuation, indicating that fluorescence quenching method can be utilized to assess the binding parameters of protein-like constituents in urban forestland soil and Cu(II) ions. This contrasted with previous researches about protein-like constituents existed in surface water (Yamashita and Jaffé 2008) and municipal solid waste leachate (Wu et al. 2011), in which distinct fluctuations were detected in the quenching curves with addition of Cu(II) ions. Therefore, although DOM in urban forestland soil showed similar fluorescent features to those of protein-like constituents, the intrinsic structures might be variable among different types of samples, thus affecting their quenching properties. In addition, the quenching phenomena with the addition of Ni(II) and Pb(II) ions could not be detected by traditional visual peaking method, demonstrating that EEM-PARAFAC modeling can provide complexation information at a deeper level, which might be neglected when using visual peak finding method due to prominent overlapping fluorescent components.

Binding parameters of different types of DOM constituents

The stability constants (K_M) and the fraction of the binding fluorescent constituents (f) for the identified constituents and four HMs were fitted applying the Ryan and Weber model (as showed in Table 4). For Cu(II) ions, the log K_M values were 5.31, 4.92, 5.72, and 4.90, respectively, which were in the reasonable range as those determined for agricultural soil DOM (Knoth de Zarruk et al. 2007), natural water DOM (Ryan and Weber 1982b), and lake sediments DOM samples (Xu et al. 2013). Being compared to the protein-like constituents, the higher stability constants between humic-like/fulvic-like constituents and Cu(II) ions may be related to the existence of great number of aromatic acidic functional groups (phenolic sites) (Martins and Drakenberg 1982). With respected to Ni(II) and Pb(II) ions, the binding parameters for C2 and C3 can be modeled well, whereas those for C1 and C4 cannot be modeled successfully, even if inconspicuous quenching phenomena were detected (Fig. 4a, d). These interesting results revealed that the binding mechanisms between

Table 4 The log K_M values for the PARAFAC constituents in urban forestland soil with four target HMs determined by Ryan and Weber model

Metals	Constituent 1			Constituent 2			Constituent 3			Constituent 4		
	log K_M	f	R^2	log K_M	f	R^2	log K_M	f	R^2	log K_M	f	R^2
Cu	5.31	67.01	0.99	4.92	50.17	0.99	5.72	63.02	0.97	4.90	70.05	0.98
Ni	FM			4.69	52.30	0.99	5.01	43.75	0.98	FM		
Pb	FM			4.37	57.01	0.92	4.69	63.89	0.98	FM		
Cd	FM				FM			FM		FM		

Ni(II)/Pb(II) ions and different types of constituents may be different. The log K_M values for Ni-C3 complex (5.01) and Pb-C3 complex (4.69) complexes were higher than Ni-C2 (4.69) and Pb-C2 (4.37) complexes, which may be attributed to the more condensed structures of C3. Furthermore, despite the EEM quenching curves of fulvic-like and humic-like constituents displayed a distinct downtrend with Cd(II) addition, the fitting results proved that the binding parameters between the four identified constituents and Cd(II) might not be analyzed reasonably through the 1:1 complex reaction model. This finding was consistent with the complexing characteristics of Cd(II) with DOM extracted from landfill leachate (Wu et al. 2011), compost-derived DOM (Xu et al. 2013), and commercial fulvic acid (Grassi and Daquino 2005).

It was noteworthy that the order of log K_M values was Cu-DOM > Ni-DOM > Pb-DOM complexes. This result can be explained as Cu(II) and Ni(II) ions may forcefully interact with DOM through the generation of comparatively stable inner-sphere complexes, where Pb(II) ions were expected to generate outer-sphere complexes to a larger extent (Hernández et al. 2006; Senesi and Loffredo 1999). In addition, the organic functional groups with strong complexing capacity usually exist in lower concentrations, whereas the organic functional groups with weak complexing capacity are present in higher concentrations (Benedetti et al. 1995; Wu and Tanoue 2001). The proportion of metal to DOM ("metal concentration effect") is known to influence the affinity of metal-DOM. For example, Cu(II) ions incline to bind with strongest ligands (nitrogen- and sulfur-containing functional groups) of DOM at low Cu/DOM ratios (generally $\leq 10^{-3}$) (Croué et al. 2003, Frenkel et al. 2000). Moreover, according to the Hard-Soft-Acid-Base theory (Haitzer et al. 2002), this effect was believed to be powerful for Ni(II) and Pb(II) due to their "hard-medial-soft" property and the low content of "soft" ligands compared to the high concentration of "hard" oxygen ligands in DOM. In this study, all the minimum initial values of Cu/DOM, Ni/DOM, and Pb/DOM were approximately 0.05, resulting in a rapid saturation of the powerful binding sites and that the most of the above three HMs tended to bind the weak sites, such as hydroxyl, phenolic, carboxylic, and carbonyl. Therefore, the log K_M values fitted by the quenching curves should be regarded as theoretical averaged constants.

FM: failed to be modeled.

Risk assessment of soil environments

EEM-PARAFAC had been shown to discriminate urban forestland soil–derived DOM into various significative components and evaluate the relative abundances of these different organic substances. Since PARAFAC modeling has the ability to determine the binding parameters of the identified organic constituents with HMs, it is possible to assess the complexation information of metal-DOM speciation in greater details. Moreover, as diffusely recognized, DOM plays a vital role in the biotoxicity and transportation of HMs in soil environments (Huang et al. 2019; Kalbitz and Wennrich 1998; Uchimiya et al. 2010; Weng et al. 2002). A relatively stronger binding ability in the existence of DOM indicated that urban forestland soil played a more significant role in the detoxification of HMs. The toxicity of HMs may be weakened after complexing with different types of ligands (Sheng et al. 2013). However, recent researchers demonstrated that elevated HM concentrations in soil could be attributed to stormwater runoff, groundwater flow, atmospheric cycling, vehicle exhaust, waste disposal, and industrial emission (Hou et al. 2017). Therefore, based on the strong metal-DOM affinity found in this study, it was deduced that the contamination of HMs in urban forestland soil might become more terrible due to inadequate control of pollution sources and neglect of maintenance for soil quality.

In addition, the content level and the chemical composition of DOM should be considered as the dominating factors in evaluating the risk of HMs in urban forestland soil environments. Previous studies on risk evaluation of HMs in soil were primarily concentrated on the total concentration and speciation, applying multiple statistical methods (principal component analysis, cluster analysis, Pearson correlation analysis, etc.) to identify the soil properties (Ali et al. 2016; Huang et al. 2015; Kelepertzis 2014). The various quenching behaviors of Cu(II), Cd(II), Pb(II), and Ni(II) found in this study suggested that the strength of complexing interaction should also be regarded as the risk assessment of HMs. Furthermore, EEM-PARAFAC model and titration results revealed that the highest binding affinity was Cu-DOM, followed by Ni-DOM, and the worst was Pb-DOM (the log K_M values of Cd-DOM cannot be obtained). Therefore, Pb(II) or Cd(II) may present a stronger toxicity in urban forestland soil ecosystems due to its relative low binding capacities and thus their toxicity should not be ignored for engineering and scientific researchers.

Conclusions

In this study, urban forestland soil samples in Daxing District were scientifically sampled with the help of GIS technology. The UV-vis and fluorescence characteristics showed that the DOM in urban forestland soil contained a complex mixture of terrestrial and microbially derived organic substances with smaller molecular weight and more aromatic structures. EEM and PARAFAC analyses were combined to study the binding affinity of HMs to urban forestland soil DOM. Four independent fluorescent constituents (1 fulvic-like, 2 humic-like, and 1 proteins-like) were decomposed by the PARAFAC model. Being compared to protein-like constituents, the binding ability of fulvic-/humic-like constituents with Cu(II) ions were relatively stronger. Considering that the Ryan and Weber

model only successfully calculated the binding parameters of Ni(II)/Pb(II) ions and humic-like constituents thus indicate that their corresponding complexes exhibited higher stability constants than the fulvic-like and protein-like constituents. Recognizing the vital role that DOM in urban forestland soil can influence the mobility, bioavailability, and toxicity of HMs, plentiful strategies should be proposed for the management of urban forestland soil microenvironments. The above results provided a detailed theoretical bias of the binding affinities of HMs and the different types of DOM at the molecular level, which was pivotal for efficient control of the transportation and transformation of HMs in urban forestland soil.

Funding information The authors received financial support from Project of Construction of Innovation Teams and Teacher Career Development for Universities and Colleges Under Beijing Municipality (IDHT20170508), Great Wall Scholars Training Program Project of Beijing Municipality Universities (CIT&TCD20180323), Beijing Talent Project (2018A35), the Fundamental Research Funds for Beijing Universities of Civil Engineering and Architecture (X18075/X18076/X18124/X18125/X18276), and the Scientific Research Foundation of Beijing University of Civil Engineering and Architecture (KYJJ2017033/KYJJ2017008).

References

Ali MH, Mustafa A-RA, El-Sheikh AA (2016) Geochemistry and spatial distribution of selected heavy metals in surface soil of Sohag, Egypt: a multivariate statistical and GIS approach. Environ Earth Sci 75: 1257–1274

Al-Khashman OA, Shawabkeh RA (2006) Metals distribution in soils around the cement factory in southern Jordan. Environ Pollut 140: 387–394

Ashworth DJ, Alloway BJ (2004) Soil mobility of sewage sludge-derived dissolved organic matter, copper, nickel and zinc. Environ Pollut 127:137–144

Bai YC, Wu FC, Liu CQ, Li W, Guo JY, Fu PQ, Xing BS, Zheng J (2008) Ultraviolet absorbance titration for determining stability constants of humic substances with Cu(II) and Hg(II). Anal Chim Acta 616:115–121

Beiyuan J, Tsang DCW, Bolan NS, Baek K, Ok YS, Li X-D (2018) Interactions of food waste compost with metals and metal-chelant complexes during soil remediation. J Clean Prod 192:199–206

Benedetti MF, Milne CJ, Kinniburgh DG, Van Riemsdijk WH, Koopal LK (1995) Metal ion binding to humic substances: application of the non-ideal competitive adsorption model. Environ Sci Technol 29: 446–457

Bianchi TS (2011) The role of terrestrially derived organic carbon in the coastal ocean: a changing paradigm and the priming effect. Proc Natl Acad Sci 108:19473–19481

Chen Z, Li Y, Pan J (2004) Distributions of colored dissolved organic matter and dissolved organic carbon in the Pearl River Estuary, China. Cont Shelf Res 24:1845–1856

Chen X, Xia X, Zhao Y, Zhang P (2010) Heavy metal concentrations in roadside soils and correlation with urban traffic in Beijing, China. J Hazard Mater 181:640–646

Chen WB, Smith DS, Guéguen C (2013) Influence of water chemistry and dissolved organic matter (DOM) molecular size on copper and mercury binding determined by multiresponse fluorescence quenching. Chemosphere 92:351–359

Coble PG (1996) Characterization of marine and terrestrial DOM in seawater using excitation-emission matrix spectroscopy. Mar Chem 51: 325–346

Croué JP, Benedetti MF, Violleau D, Leenheer JA (2003) Characterization and copper binding of humic and nonhumic organic matter isolated from the South Platte River: evidence for the presence of nitrogenous binding site. Environ Sci Technol 37:328–336

Del Galdo I, Six J, Peressotti A, Francesca Cotrufo M (2003) Assessing the impact of land-use change on soil C sequestration in agricultural soils by means of organic matter fractionation and stable C isotopes. Glob Chang Biol 9:1204–1213

Divya O, Venkataraman V, Mishra AK (2009) Analysis of metal ion concentration in humic acid by excitation-emission matrix fluorescence and chemometric methods. J Appl Spectrosc 76:864–875

Dudal Y, Sévenier G, Dupont L, Guillon E (2005) Fate of the metal-binding soluble organic matter throughput a soil profile. Soil Sci 170:707–715

Fang W, Wei Y, Liu J (2016) Comparative characterization of sewage sludge compost and soil: heavy metal leaching characteristics. J Hazard Mater 310:1–10

Fellman JB, D'Amore DV, Hood E, Boone RD (2008) Fluorescence characteristics and biodegradability of dissolved organic matter in forest and wetland soils from coastal temperate watersheds in southeast Alaska. Biogeochemistry 88:169–184

Fellman JB, Hood E, D'Amore DV, Edwards RT, White D (2009) Seasonal changes in the chemical quality and biodegradability of dissolved organic matter exported from soils to streams in coastal temperate rainforest watersheds. Biogeochemistry 95:277–293

Frenkel AI, Korshin GV, Ankudinov AL (2000) XANES study of Cu^{2+}-binding sites in aquatic humic substances. Environ Sci Technol 34: 2138–2142

Gao L, Zhou Z, Reyes AV, Guo L (2018) Yields and characterization of dissolved organic matter from different aged soils in Northern Alaska. J Geophys Res Biogeosci 123:2035–2052

Grassi M, Daquino V (2005) 113Cd NMR and fluorescence studies of multiple binding mechanisms of Cd(II) by the Suwannee River fulvic acid. Ann Chim Rome 95:579–591

Guo W, Stedmon CA, Han Y, Wu F, Yu X, Hu M (2007) The conservative and non-conservative behavior of chromophoric dissolved organic matter in Chinese estuarine waters. Mar Chem 107:357–366

Haitzer M, Aiken GR, Ryan JN (2002) Binding of mercury(II) to dissolved organic matter: the role of the mercury-to-DOM concentration ratio. Environ Sci Technol 36:3564–3570

Hassouna M, Théraulaz F, Massiani C (2012) Production and elimination of water extractable organic matter in a calcareous soil as assessed by UV/Vis absorption and fluorescence spectroscopy of its fractions isolated on XAD-8/4 resins. Geoderma 189-190:404–414

Helms JR, Stubbins A, Ritchie JD, Minor EC, Kieber DJ, Mopper K (2008) Absorption spectral slopes and slope ratios as indicators of molecular weight, source, and photobleaching of chromophoric dissolved organic matter. Limnol Oceanogr 53:955–969

Hernández D, Plaza C, Senesi N, Polo A (2006) Detection of copper(II) and zinc(II) binding to humic acids from pig slurry and amended soils by fluorescence spectroscopy. Environ Pollut 143:212–220

Hong H, Yang L, Guo W, Wang F, Yu X (2012) Characterization of dissolved organic matter under contrasting hydrologic regimes in a subtropical watershed using PARAFAC model. Biogeochemistry 109:163–174

Hong J, Xie H, Guo L, Song G (2014) Carbon monoxide photoproduction: implications for photoreactivity of arctic permafrost-derived soil dissolved organic matter. Environ Sci Technol 48:9113–9121

Hou D, O'Connor D, Nathanail P, Tian L, Ma Y (2017) Integrated GIS and multivariate statistical analysis for regional scale assessment of heavy metal soil contamination: a critical review. Environ Pollut 231:1188–1200

Huang Y, Li T, Wu C, He Z, Japenga J, Deng M, Yang X (2015) An integrated approach to assess heavy metal source apportionment in peri-urban agricultural soils. J Hazard Mater 299:540–549

Huang M, Li Z, Huang B, Luo N, Zhang Q, Zhai X, Zeng G (2018) Investigating binding characteristics of cadmium and copper to DOM derived from compost and rice straw using EEM-PARAFAC combined with two-dimensional FTIR correlation analyses. J Hazard Mater 344:539–548

Huang M, Li Z, Luo N, Yang R, Wen J, Huang B, Zeng G (2019) Application potential of biochar in environment: insight from degradation of biochar-derived DOM and complexation of DOM with heavy metals. Sci Total Environ 646:220–228

Huguet A, Vacher L, Relexans S, Saubusse S, Froidefond JM, Parlanti E (2009) Properties of fluorescent dissolved organic matter in the Gironde Estuary. Org Geochem 40:706–719

Huguet A, Vacher L, Saubusse S, Etcheber H, Abril G, Relexans S, Ibalot F, Parlanti E (2010) New insights into the size distribution of fluorescent dissolved organic matter in estuarine waters. Org Geochem 41:595–610

Hunt JF, Ohno T (2007) Characterization of fresh and decomposed dissolved organic matter using excitation-emission matrix fluorescence spectroscopy and multiway analysis. J Agric Food Chem 55:2121–2128

Hur J, Lee B-M (2011) Characterization of binding site heterogeneity for copper within dissolved organic matter fractions using two-dimensional correlation fluorescence spectroscopy. Chemosphere 83:1603–1611

Ishii SKL, Boyer TH (2012) Behavior of reoccurring PARAFAC components in fluorescent dissolved organic matter in natural and engineered systems: a critical review. Environ Sci Technol 46: 2006–2017

Jiang J, Yu H, Xi B, Meng F, Zhou Y, Liu H (2012) UV-visible spectroscopic properties of dissolved fulvic acids extracted from salined fluvo-aquic soils in the Hetao Irrigation District, China. Soil Res 49:670–679

Jiang T, Skyllberg U, Björn E, Green NW, Tang J, Wang D, Gao J, Li C (2017) Characteristics of dissolved organic matter (DOM) and relationship with dissolved mercury in Xiaoqing River-Laizhou Bay estuary, Bohai Sea, China. Environ Pollut 223:19–30

Jordan RN, Yonge DR, Hathhorn WE (1997) Enhanced mobility of Pb in the presence of dissolved natural organic matter. J Contam Hydrol 29:59–80

Kalbitz K, Wennrich R (1998) Mobilization of heavy metals and arsenic in polluted wetland soils and its dependence on dissolved organic matter. Sci Total Environ 209:27–39

Kelepertzis E (2014) Accumulation of heavy metals in agricultural soils of Mediterranean: insights from argolida basin, Peloponnese, Greece. Geoderma 221-222:82–90

Knoth de Zarruk K, Scholer G, Dudal Y (2007) Fluorescence fingerprints and Cu^{2+}-complexing ability of individual molecular size fractions in soil- and waste-borne DOM. Chemosphere 69:540–548

Korshin GV, Li CW, Benjamin MM (1997) Monitoring the properties of natural organic matter through UV spectroscopy: a consistent theory. Water Res 31:1787–1795

Kumar GP, Yadav SK, Thawale PR, Singh SK, Juwarkar AA (2008) Growth of Jatropha curcas on heavy metal contaminated soil amended with industrial wastes and Azotobacter-a greenhouse study. Bioresour Technol 99:2078–2082

Lee CS, Li X, Shi W, Shi W, Cheung SC, Thornton I (2006) Metal contamination in urban, suburban, and country park soils of Hong Kong: a study based on GIS and multivariate statistics. Sci Total Environ 356:45–61

Lee B-M, Seo Y-S, Hur J (2015) Investigation of adsorptive fractionation of humic acid on graphene oxide using fluorescence EEM-PARAFAC. Water Res 73:242–251

Li P, Hur J (2017) Utilization of UV-vis spectroscopy and related data analyses for dissolved organic matter (DOM) studies: a review. Crit Rev Environ Sci Technol 47:131–154

Li Q, Guo X, Chen L, Li Y, Yuan D, Dai B, Wang S (2017) Investigating the spectral characteristic and humification degree of dissolved organic matter in saline-alkali soil using spectroscopic techniques. Front Earth Sci 11:76–84

Li G, Khan S, Ibrahim M, Sun T-R, Tang J-F, Cotner JB, Xu Y-Y (2018a) Biochars induced modification of dissolved organic matter (DOM) in soil and its impact on mobility and bioaccumulation of arsenic and cadmium. J Hazard Mater 348:100–108

Li S, Yn C, Zhang J, Song K, Mu G, Sun C, Ju H, Ji M (2018b) The relationship of chromophoric dissolved organic matter parallel factor analysis fluorescence and polycyclic aromatic hydrocarbons in natural surface waters. Environ Sci Pollut Res 25:1428–1438

Lind T, Valmari T, Kauppinen EI, Sfiris G, Nilsson K, Maenhaut W (1999) Volatilization of the heavy metals during circulating fluidized bed combustion of forest residue. Environ Sci Technol 33:496–502

Liu S-Y, Xu J, Chen W-L, David BE, Wu M, Ma F (2017) Impacts of potassium ferrate(VI) on the growth and organic matter accumulation, production, and structural changes in the cyanobacterium Microcystis aeruginosa. Environ Sci Pollut Res 24:11299–11308

Luo C, Liu C, Wang Y, Liu X, Li F, Zhang G, Li X (2011) Heavy metal contamination in soils and vegetables near an e-waste processing site, south China. J Hazard Mater 186:481–490

Martins EO, Drakenberg T (1982) Cadmium(II), zinc(II), and copper(II) ions binding to bovine serum albumin. A 113Cd NMR study. Inorg Chim Acta 67:71–74

Mcknight DM, Boyer EW, Westerhoff PK, Doran PT, Kulbe T, Andersen DT (2001) Spectrofluorometric characterization of dissolved organic matter for indication of precursor organic material and aromaticity. Limnol Oceanogr 46:38–48

Meza-Figueroa D, De la O-Villanueva M, De la Parra ML (2007) Heavy metal distribution in dust from elementary schools in Hermosillo, Sonora, México. Atmos Environ 41:276–288

Mignone RA, Martin MV, Morán Vieyra FE, Palazzi VI, López de Mishima B, Mártire DO, Borsarelli CD (2012) Modulation of optical properties of dissolved humic substances by their molecular complexity. Photochem Photobiol 88:792–800

Mounier S, Zhao H, Garnier C, Redon R (2011) Copper complexing properties of dissolved organic matter: PARAFAC treatment of fluorescence quenching. Biogeochemistry 106:107–116

Nierop KG, Jansen B, Verstraten JM (2002) Dissolved organic matter, aluminium and iron interactions: precipitation induced by metal/carbon ratio, pH and competition. Sci Total Environ 300:201–211

O'Donnell JA, Aiken GR, Butler KD, Guillemette F, Podgorski DC, Spencer RGM (2016) DOM composition and transformation in boreal forest soils: the effects of temperature and organic-horizon decomposition state. J Geophys Res Biogeosci 121:2727–2744

Ohno T (2002) Fluorescence inner-filtering correction for determining the humification index of dissolved organic matter. Environ Sci Technol 36:742–746

Ohno T, Amirbahman A, Bro R (2008) Parallel factor analysis of excitation-emission matrix fluorescence spectra of water soluble soil organic matter as basis for the determination of conditional metal binding parameters. Environ Sci Technol 42:186–192

Ohno T, He Z, Sleighter RL, Honeycutt CW, Hatcher PG (2010) Ultrahigh resolution mass spectrometry and indicator species analysis to identify marker components of soil- and plant biomass-derived organic matter fractions. Environ Sci Technol 44:8594–8600

Peuravuori J, Pihlaja K (2004) Preliminary study of lake dissolved organic matter in light of nanoscale supramolecular assembly. Environ Sci Technol 38:5958–5967

Phong DD, Hur J (2015) Insight into photocatalytic degradation of dissolved organic matter in UVA/TiO_2 systems revealed by fluorescence EEM-PARAFAC. Water Res 87:119–126

Refaey Y, Jansen B, De Voogt P, Parsons JR, El-Shater A-H, El-Haddad A-A, Kalbitz K (2017) Influence of organo-metal interactions on regeneration of exhausted clay mineral sorbents in soil columns loaded with heavy metals. Pedosphere 27:579–587

Romera-Castillo C, Chen M, Yamashita Y, Jaffé R (2014) Fluorescence characteristics of size-fractionated dissolved organic matter: implications for a molecular assembly based structure? Water Res 55:40–51

Ryan DK, Weber JH (1982a) Fluorescence quenching titration for determination of complexing capacities and stability constants of fulvic acid. Anal Chem 54:986–990

Ryan DK, Weber JH (1982b) Copper(II) complexing capacities of natural waters by fluorescence quenching. Environ Sci Technol 16:866–872

Santos PSM, Otero M, Duarte RMBO, Duarte AC (2009) Spectroscopic characterization of dissolved organic matter isolated from rainwater. Chemosphere 74:1053–1061

Santos PSM, Santos EBH, Duarte AC (2012) First spectroscopic study on the structural features of dissolved organic matter isolated from rainwater in different seasons. Sci Total Environ 426:172–179

Senesi N, Loffredo E (1999) The chemistry of soil organic matter. Taylor & Francis Group

Sheng G-P, Xu J, Luo H-W, Li W-W, Li W-H, Yu H-Q, Xie Z, Wei S-Q, Hu F-C (2013) Thermodynamic analysis on the binding of heavy metals onto extracellular polymeric substances (EPS) of activated sludge. Water Res 47:607–614

Six J, Guggenberger G, Paustian K, Haumaier L, Elliott ET, Zech W (2002) Sources and composition of soil organic matter fractions between and within soil aggregates. Eur J Soil Sci 52:607–618

Spencer RGM, Butler KD, Aiken GR (2012) Dissolved organic carbon and chromophoric dissolved organic matter properties of rivers in the USA. J Geophys Res Biogeosci 117:3001–3014

Stedmon CA, Bro R (2008) Characterizing dissolved organic matter fluorescence with parallel factor analysis: a tutorial. Limnol Oceanogr 6:572–579

Stedmon CA, Markager S (2001) The optics of chromophoric dissolved organic matter (CDOM) in the Greenland Sea: an algorithm for differentiation between marine and terrestrially derived organic matter. Limnol Oceanogr 46:2087–2093

Stedmon CA, Markager S (2005) Resolving the variability in dissolved organic matter fluorescence in a temperate estuary and its catchment using PARAFAC analysis. Limnol Oceanogr 50:686–697

Stedmon CA, Markager S, Bro R (2003) Tracing dissolved organic matter in aquatic environments using a new approach to fluorescence spectroscopy. Mar Chem 82:239–254

Struthers H, Spingler B, Mindt TL, Schibli R (2008) "Click-to-chelate": design and incorporation of triazole-containing metal-chelating systems into biomolecules of diagnostic and therapeutic interest. Chemistry 14:6173–6183

Stumpe B, Marschner B (2010) Dissolved organic carbon from sewage sludge and manure can affect estrogen sorption and mineralization in soils. Environ Pollut 158:148–154

Sun F, Polizzotto ML, Guan D, Wu J, Shen Q, Ran W, Wang B, Yu G (2017) Exploring the interactions and binding sites between Cd and functional groups in soil using two-dimensional correlation spectroscopy and synchrotron radiation based spectromicroscopies. J Hazard Mater 326:18–25

Uchimiya M, Lima IM, Thomas Klasson K, Chang S, Wartelle LH, Rodgers JE (2010) Immobilization of heavy metal ions (Cu^{II}, Cd^{II}, Ni^{II}, and Pb^{II}) by broiler litter-derived biochars in water and soil. J Agric Food Chem 58:5538–5544

Wang Z, Cao J, Meng F (2015) Interactions between protein-like and humic-like components in dissolved organic matter revealed by fluorescence quenching. Water Res 68:404–413

Wang H, Yuan X, Wu Y, Zeng G, Dong H, Chen X, Leng L, Wu Z, Peng L (2016) In situ synthesis of In_2S_3@MIL-125(Ti) core-shell microparticle for the removal of tetracycline from wastewater by integrated adsorption and visible-light-driven photocatalysis. Appl Catal B Environ 186:19–29

Wang H, Wu Y, Feng M, Tu W, Xiao T, Xiong T, Ang H, Yuan X, Chew JW (2018a) Visible-light-driven removal of tetracycline antibiotics and reclamation of hydrogen energy from natural water matrices and wastewater by polymeric carbon nitride foam. Water Res 144:215–225

Wang H, Wu Y, Xiao T, Yuan X, Zeng G, Tu W, Wu S, Lee HY, Tan YZ, Chew JW (2018b) Formation of quasi-core-shell In_2S_3/anatase TiO2@metallic $Ti_3C_2T_x$ hybrids with favorable charge transfer channels for excellent visible-light-photocatalytic performance. Appl Catal B Environ 233:213–225

Ward NI, Brooks RR, Roberts E, Boswell CR (1977) Heavy-metal pollution from automotive emissions and its effect on roadside soils and pasture species in New Zealand. Environ Sci Technol 11:917–920

Wei B, Yang L (2010) A review of heavy metal contaminations in urban soils, urban road dusts and agricultural soils from China. Microchem J 94:99–107

Weng L, Temminghoff EJM, Lofts S, Tipping E, Van Riemsdijk WH (2002) Complexation with dissolved organic matter and solubility control of heavy metals in a sandy soil. Environ Sci Technol 36:4804–4810

Wu F, Tanoue E (2001) Isolation and partial characterization of dissolved copper-complexing ligands in streamwaters. Environ Sci Technol 35:3646–3652

Wu LH, Luo YM, Christie P, Wong MH (2003) Effects of EDTA and low molecular weight organic acids on soil solution properties of a heavy metal polluted soil. Chemosphere 50:819–822

Wu F, Evans D, Dillon P, Schiff S (2004) Molecular size distribution characteristics of the metal-DOM complexes in stream waters by high-performance size-exclusion chromatography (HPSEC) and high-resolution inductively coupled plasma mass spectrometry (ICP-MS). J Anal Atom Spectrom 19:979–983

Wu J, Zhang H, He P-J, Shao L-M (2011) Insight into the heavy metal binding potential of dissolved organic matter in MSW leachate using EEM quenching combined with PARAFAC analysis. Water Res 45:1711–1719

Wu J, Zhang H, Yao Q-S, Shao L-M, He P-J (2012) Toward understanding the role of individual fluorescent components in DOM-metal binding. J Hazard Mater 215-216:294–301

Xu H, Yu G, Yang L, Jiang H (2013) Combination of two-dimensional correlation spectroscopy and parallel factor analysis to characterize the binding of heavy metals with DOM in lake sediments. J Hazard Mater 263:412–421

Yamashita Y, Jaffé R (2008) Characterizing the interactions between trace metals and dissolved organic matter using excitation-emission matrix and parallel factor analysis. Environ Sci Technol 42:7374–7379

Yang J, McBride J, Zhou J, Sun Z (2005) The urban forest in Beijing and its role in air pollution reduction. Urban For Urban Gree 3:65–78

Yang JY, Yang XE, He ZL, Li TQ, Shentu JL, Stoffella PJ (2006) Effects of pH, organic acids, and inorganic ions on lead desorption from soils. Environ Pollut 143:9–15

Yang L, Chang SW, Shin HS, Hur J (2015) Tracking the evolution of stream DOM source during storm events using end member mixing analysis based on DOM quality. J Hydrol 523:333–341

Ye C, Li S, Zhang Y, Zhang Q (2011) Assessing soil heavy metal pollution in the water-level-fluctuation zone of the Three Gorges Reservoir, China. J Hazard Mater 191:366–372

Yu G-H, Wu M-J, Wei G-R, Luo Y-H, Ran W, Wang B-R, Jc Z, Shen Q-R (2012) Binding of organic ligands with Al(III) in dissolved organic

matter from soil: implications for soil organic carbon storage. Environ Sci Technol 46:6102–6109

Zhao C, Wang CC, Li JQ, Wang CY, Wang P, Pei ZJ (2015) Dissolved organic matter in urban stormwater runoff at three typical regions in Beijing: chemical composition, structural characterization and source identification. RSC Adv 5:73490–73500

Zhao C, Wang CC, Li JQ, Wang CY, Zhu YR, Wang P, Zhang N (2016) Chemical characteristics of chromophoric dissolved organic matter in stormwater runoff of a typical residential area, Beijing. Desalin Water Treat 57:19727–19740

Zhao C, Wang C-C, Li J-Q, Wang P, Ou J-Q, Cui J-R (2018a) Interactions between copper(II) and DOM in the urban stormwater runoff: modeling and characterizations. Environ Technol 39:120–129

Zhao C, Wang Z, Wang C, Li X, Wang C-C (2018b) Photocatalytic degradation of DOM in urban stormwater runoff with TiO_2 nanoparticles under UV light irradiation: EEM-PARAFAC analysis and influence of co-existing inorganic ions. Environ Pollut 243: 177–188

Zhou A, Du J, Varrone C, Wang Y, Wang A, Liu W (2014) VFAs bioproduction from waste activated sludge by coupling pretreatments with Agaricus bisporus substrates conditioning. Process Biochem 49:283–289

Zhou Y, Jeppesen E, Zhang Y, Shi K, Liu X, Zhu G (2016) Dissolved organic matter fluorescence at wavelength 275/342 nm as a key indicator for detection of point-source contamination in a large Chinese drinking water lake. Chemosphere 144:503–509

Zhu B, Pennell SA, Ryan DK (2014) Characterizing the interaction between uranyl ion and soil fulvic acid using parallel factor analysis and a two-site fluorescence quenching model. Microchem J 115:51–57